

Large-scale first principles configuration interaction calculations of optical absorption in aluminum clusters

Ravindra Shinde* and Alok Shukla†

Department of Physics, Indian Institute of Technology Bombay, Mumbai, Maharashtra 400076, INDIA.

We report the linear optical absorption spectra of aluminum clusters Al_n ($n=2-5$), using systematic large-scale all-electron correlated calculations. Several low-lying isomers of each cluster were considered, and their geometries were optimized at the coupled-cluster singles doubles (CCSD) level of theory. With these optimized ground-state geometries, excited states of different clusters were computed using the multi-reference singles-doubles configuration-interaction (MRSDCI) approach, which includes electron correlation effects at a sophisticated level. These CI wave functions were used to compute the transition dipole matrix elements connecting the ground and various excited states of different clusters, eventually leading to their linear absorption spectra. The convergence of our results with respect to the basis sets, and the size of the CI expansion, was carefully examined. The contribution of configurations to many body wavefunction of various excited states suggests that the excitations involved are collective, and plasmonic in nature.

PACS numbers: 36.40.Vz, 36.40.Mr, 31.15.V-, 31.15.vj

I. INTRODUCTION

Metal clusters are promising candidates in the era of nanotechnology. The reason behind growing interest in this field lies in interesting properties, applicability of very simple theoretical models to describe their properties, and a vast variety of potential technological applications [1–5].

Various jellium models have successfully described electronic structures of alkali metal clusters, because alkali metals have free valence electrons. This beautifully explains the magic abundance of certain clusters. However, in case of aluminum clusters, the experimental results often provide conflicting evidence about the size at which the jellium model would work. The theoretical explanation also depends on the valency of aluminum atoms considered. Since $s - p$ orbital energy separation in aluminum atom is 4.99 eV, and it decreases with the cluster size, the valency should be changed from one to three [6]. Perturbed jellium model, which takes orbital anisotropy into account, has successfully explained the mass abundance of aluminum clusters [7, 8].

Shell structure and $s - p$ hybridization in anionic aluminum clusters were probed using photoelectron spectroscopy by Grantefer and Eberhardt [9], and Li *et al.* [10]. Evolution of electronic structure and other properties of aluminum clusters has been studied in many reports [6, 7, 10–20]. Structural properties of aluminum clusters were studied using density functional theory by Rao and Jena [6]. An all electron and model core potential study were carried out by Martinez *et al.* [19]. Upton performed chemisorption calculations on aluminum clusters and reported that Al_6 will be the smallest cluster that will absorb H_2 . DFT alongwith molecular dynamics

were used to study electronic and structural properties of aluminum clusters [16].

The optical absorption in alkali metal clusters has been studied extensively at various levels of theory [21–24]. On the contrary, although there is enormous information available about ground state structures, very little information is available about excited states of aluminum clusters. Optical absorption in several aluminum clusters corresponding to the minimum energy configurations has been studied by Deshpande *et al.* using time-dependent density functional theory (TDDFT) [25]. Xie *et al.* presented TDDFT optical absorption spectra of various caged icosahedral aluminum clusters [26]. However, no theoretical or experimental study has been done on optical absorption in various low lying isomers of aluminum clusters. The distinction of different isomers of a cluster has to be made using an experimental or theoretical technique in which the properties are size, as well as shape, dependent. Conventional mass spectrometry only distinguishes clusters according to the masses. Hence, our technique can be coupled with the experimental measurements of optical absorption to distinguish between different isomers of a cluster. We have recently reported results of such calculation on small boron clusters [27].

In this paper, we present results of systematic calculations of optical absorption in various low lying isomers of small aluminum clusters using *ab initio* large-scale configuration interaction method. The nature of optical excitations involved in absorption have also been presented by analyzing the wave functions of the excited states.

Remainder of the paper is organized as follows. Next section discusses theoretical and computational details of the calculations, followed by section III, in which results are presented and discussed. Conclusions and future directions are presented in section IV. Paper ends with an appendix presenting detailed information about wavefunctions of excited states contributing to various photoabsorption peaks.

* Corresponding author: ravindra.shinde@iitb.ac.in

† shukla@phy.iitb.ac.in

II. THEORETICAL AND COMPUTATIONAL DETAILS

The geometry of various isomers were optimized using the size-consistent coupled-cluster singles-doubles (CCSD) method, as implemented in the Gaussian 09 package [28]. A basis set of 6-311++G(2d,2p) was used which was included in the Gaussian 09 package itself. This basis set is optimized for the ground state calculations. Since an even numbered electron system can have singlet, triplet, or higher spin multiplicity, we repeated the optimization for singlet and triplet systems to look for true ground state geometry. Similarly, for odd numbered electron systems, doublet and quartet multiplicities were considered in the geometry optimization. To initiate the optimization, raw geometries, reported by Rao and Jena, based on density functional method were used [6]. Figure 1 shows the final optimized geometries of the isomers studied in this paper.

Using these optimized geometries, correlated calculations were performed using multireference singles doubles configuration interaction (MRSDCI) method for both ground state and excited states [29]. This method considers a large number of singly- and doubly- substituted configurations from a large number of reference configurations, and, is well suited for both ground and excited states calculations. It takes into account the electron correlation which is inadequately represented in single reference *ab initio* methods. These ground- and excited-state wavefunctions are further used to calculate the transition dipole moment matrix elements, which in turn, are utilized to compute linear optical absorption spectrum assuming a Lorentzian line shape.

Various wave functions of the excited states contributing to the peaks in the spectrum were analyzed, and even bigger MRSDCI calculations were performed by including more references, if needed. The criteria of choosing a reference in the calculation was based upon the magnitude of the corresponding coefficients in the CI wave function of the excited states contributing to a peak in the spectrum. This process was repeated until the spectrum converges within acceptable tolerance and all the configurations which contribute to various excited states were included. The typical number of reference configurations and total number of configurations considered in the calculations of various isomers are given in Table I. We have extensively used such approach in performing large-scale correlated calculations of linear optical absorption spectra of conjugated polymers [30–33], and atomic clusters [27].

Since configuration interaction method is computationally very expensive, mainly, because the number of determinants to be considered increases exponentially with the number of electrons, and the number of molecular orbitals. Calculations on bigger clusters are prohibitive under such circumstances, and are very time consuming even for the clusters considered here. Therefore, whenever possible, efforts were made to minimize

the computational time by using systems properties and some approximations. Point group symmetries (D_{2h} , and its subgroups) were taken into account, thereby making calculations for each symmetry subspace independent of each other. The core of the aluminum atom were frozen from excitations, keeping only three valence electrons active. Also an upper limit on the number of virtual orbitals was imposed, to restrict very high energy excitations. The effect of these approximations on the computed photoabsorption spectra has been studied carefully and is presented in the next section.

III. RESULTS AND DISCUSSION

In this section, we have presented a systematic study of the convergence of our results and various approximations used. In the latter part, we discuss the results of our calculations of various clusters.

A. Convergence of calculations

In this section we discuss the convergence of photoabsorption calculations with respect to the choice of the basis set, and the size of the active orbital space.

1. Choice of basis set

It is well known that, electronic structure calculations are basis set dependent. Several basis sets are optimized for specific purposes, such as ground state calculations, excited states and covalent systems etc. We have reported a systematic basis set dependence of photoabsorption of boron cluster [27]. Similarly, here we have checked the dependence of photoabsorption spectrum of aluminum dimer on basis sets used [34, 35] as shown in Fig. 2. The 6-311 type Gaussian contracted basis sets are known to be good for ground state calculations. The correlation consistent (CC) basis sets, namely, CC-polarized valence double-zeta and CC-polarized valence triple zeta (cc-pVTZ) give a good description of excited states of systems. The latter is found to be more sophisticated in describing the high energy excitations, which were also confirmed using results of an independent TDDFT calculation [36]. So we have used cc-pVTZ basis set for the optical absorption calculations.

2. Orbital truncation scheme

With respect to the total number of orbitals N in the system, the computational time in configuration interaction calculations scales as $\approx N^6$. Therefore such calculations become intractable for moderately sized systems, such as those considered here. So, in order to ease those

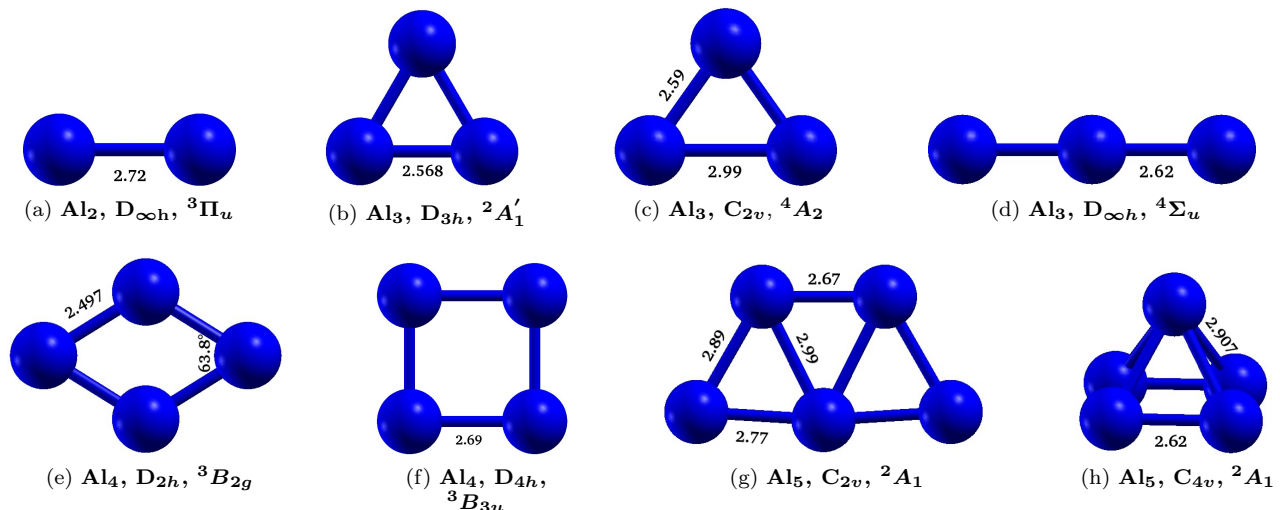


Figure 1: (Color online) Geometry optimized structures of aluminum clusters with point group symmetry and the electronic ground state at the CCSD level. All numbers are in Å unit.

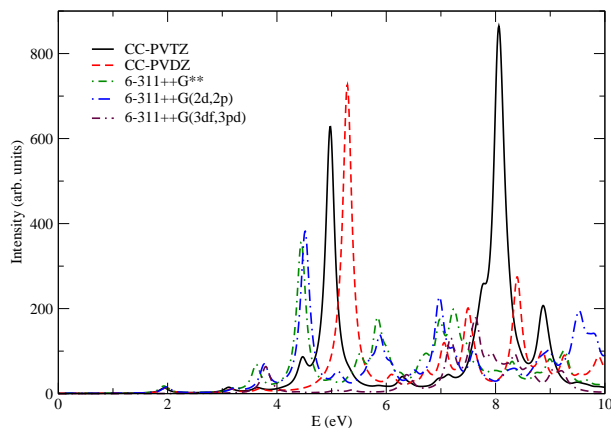


Figure 2: (Color online) Optical absorption in Al_2 calculated using various Gaussian contracted basis sets.

calculations, the lowest lying molecular orbitals are constrained to be doubly occupied in all the configurations, implying that no optical excitation can occur from those orbitals. It reduces the size of the CI Hamiltonian matrix drastically. In fact, this approach is recommended in quantum chemical calculations, because the basis sets used are not optimized to incorporate the correlations in core electrons [37]. The effect of this approximation on the spectrum is as shown in Fig. 3. Since, calculations with all electrons in active orbitals were unfeasible, we have frozen occupied orbitals upto -4 Hartree of energy for the purpose of demonstration. The effect of freezing the core is negligibly small in the low energy regime, but shows disagreement in the higher energy range. However, for very high energy excitations, photodissociation may occur, hence absorption spectra at those energies

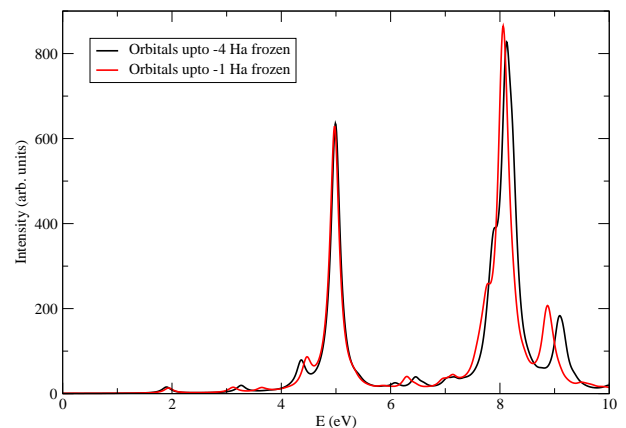


Figure 3: (Color online) The effect of freezing the core orbitals of aluminum atoms on optical absorption spectrum of Al_2 . It renders little effect on optical absorption spectrum, with significant reduction in the computational cost.

will cease to have meaning. Thus, the advantage of freezing the core subdues this issue. Therefore, in all the calculations, we have frozen the chemical core from optical excitations.

Not only occupied, but high energy virtual (unoccupied) orbitals can also be removed from the calculations to make them tractable. In this case the high lying orbitals are constrained to be unoccupied in all the configurations. This move is justifiable, because it is unlikely that electrons would prefer partial filling of high energy orbitals in an attempt to avoid other electrons. However, this will only be applicable if the orbitals are sufficiently high in energy. Fig. 4 shows the effect of removing or

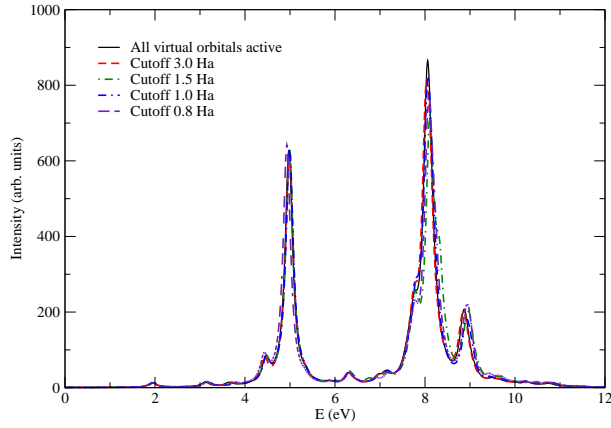


Figure 4: (Color online) The effect of the number of active orbitals (N_{act}) on the optical absorption spectrum of Al_2 . Until $N_{act}=46$, the optical spectrum does not exhibit any significant change. It corresponds to 1.0 Hartree (≈ 27.2 eV) virtual orbital energy.

bitals having more than the specified energy. From the figure it is clear that photoabsorption spectra exhibits no difference at all upto 1 Hartree cutoff on virtual orbitals. Below 0.8 Ha cutoff, the spectra start deviating from each other. Hence, we have ignored the virtual orbitals having energy more than 1 Ha.

3. Size of the CI expansion

In the multireference configuration interaction method, the size of the CI Hamiltonian increases exponentially with the number of molecular orbitals in the system. Also, accurate correlated results can only be obtained if sufficient number of reference configurations are included in the calculations. In our calculations, we have included those configurations which are dominant in the wave functions of excited states for a given absorption peak. Also, for ground state calculations, we included configurations until the total energy converges within a pre-defined tolerance. Table I shows the average number of reference configurations and average number of total configurations involved in the CI calculations of various isomers. For a given isomer, the average is calculated across different irreducible representations needed in these symmetry adapted calculations of the ground and various excited states. For the simplest cluster, the total configurations are about half a million and for the biggest cluster considered here, it is around four million for each symmetry subspace of Al_5 . The superiority of our calculations can also be judged from the correlation energy defined here (*cf.* Table I), which is the difference in the total energy of a system at the MRSDCI level and the Hartree-Fock level. The correlation energy per atom seems to be quite high for all the clusters, making our calculations stand out among other electronic structure

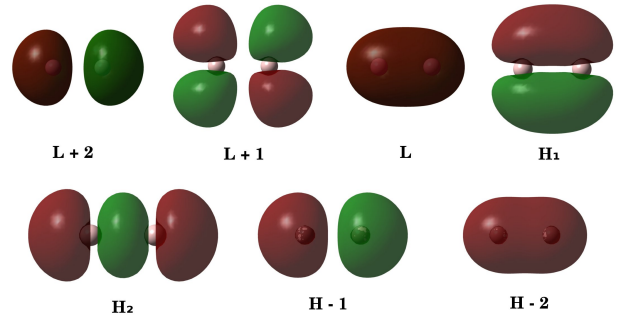


Figure 5: (Color online) Molecular orbitals of aluminum dimer. H and L stands for HOMO and LUMO respectively, and H_1 and H_2 are singly occupied degenerate molecular orbitals.

calculations, especially single reference DFT based calculations.

B. Calculated photoabsorption spectra of various clusters

In this section, we describe the photoabsorption spectra of various isomers of the aluminum clusters studied. Graphical presentation of molecular orbitals involved are also given in each subsection below.

1. Al_2

Aluminum dimer is the most widely studied cluster of aluminum. It has now been confirmed that the Al_2 (*cf.* Fig. 1(a)) has $^3\Pi_u$ ground state. The bond length obtained using geometry optimization at CCSD level was 2.72 Å with $D_{\infty h}$ point group symmetry. This is in very good agreement with available data, such as Martinez *et al.* obtained 2.73 Å as dimer length using all electron calculations [19], 2.71 Å [17] and 2.75 Å [38] as bond lengths using DFT and configuration interaction methods, and 2.86 Å obtained using DFT with generalized gradient approximation [6]. The experimental bond length of aluminum dimer is 2.70 Å [39]. Another metastable state of the dimer exists with $^3\Sigma_g^-$ electronic state, and 2.48 Å in bond length.

The many-particle wave function of Al_2 consists of two degenerate singly occupied molecular orbitals (to be denoted by H_1 and H_2 , henceforth), because it is a spin triplet system. Similarly, the configurations involving excitations from occupied molecular orbitals to the unoccupied orbitals, form excited state wave functions. The computed photoabsorption spectra of Al_2 , as shown in Fig. 6, is characterized by weaker absorption at lower energies and couple of intense peaks at higher energies. The many-particle wave functions of excited states contributing to the peaks are presented in Table A.1. The spectrum starts with a small absorption peak at around 2 eV,

Table I: The average number of reference configurations (N_{ref}), and average number of total configurations (N_{total}) involved in MRSDCI calculations, ground state (GS) energies (in Hartree) at the MRSDCI level, relative energies and correlation energies (in eV) of various isomers of aluminum clusters.

| Cluster | Isomer | N_{ref} | N_{total} | GS energy (Ha) | Relative energy (eV) | Correlation energy ^a per atom (eV) |
|-----------------|------------------------|-----------|-------------|----------------|----------------------|---|
| Al ₂ | Linear | 40 | 445716 | -483.9063281 | 0.0 | 1.69 |
| Al ₃ | Equilateral triangular | 40 | 1917948 | -725.9053663 | 0.00 | 2.38 |
| | Isosceles triangular | 22 | 1786700 | -725.8748996 | 0.83 | 2.36 |
| | Linear | 18 | 1627016 | -725.8370397 | 1.85 | 2.16 |
| Al ₄ | Rhombus | 13 | 3460368 | -967.8665897 | 0.00 | 1.82 |
| | Square | 21 | 1940116 | -967.8258673 | 1.11 | 1.80 |
| Al ₅ | Pentagonal | 7 | 3569914 | -1209.8114803 | 0.00 | 1.73 |
| | Pyramidal | 8 | 3825182 | -1209.7836568 | 0.76 | 1.77 |

^a The difference in Hartree-Fock energy and MRSDCI correlated energy of the ground state.

characterized by $H_2 \rightarrow L+1$ and light polarized along the direction of axis of the dimer. It is followed by a couple of small intensity peaks, until a dominant absorption is seen at 5 eV. This is characterized by $H_1 \rightarrow L+3$. Another dominant peak is observed at 8 eV having $H-2 \rightarrow L$ as dominant configuration, with absorption due to light polarized perpendicular to the axis of the dimer.

If we compare this spectrum with the one obtained from time-dependent local density approximation (TDLDA) method [25], we get a fair agreement - although there is disagreement with respect to the intensity and number of peaks. Unlike our calculations, the number of peaks is much more in TDLDA results and the spectrum is almost continuous. Two major peaks at 5 eV and 8 eV are in complete agreement with the previously reported results of Deshpande *et al.* [25]. Minor peaks at 3.2 eV and 6.3 eV are also observed in the TDLDA spectrum of dimer. The latter one is, contrary to TDLDA spectrum, found to be a small peak in our calculations.

2. Al₃

Among the possible isomers of aluminum cluster Al₃, the equilateral triangular isomer is found to be the most stable. We have considered three isomers of Al₃, namely, equilateral triangle, isosceles triangle, and a linear chain. The most stable isomer has D_{3h} point group symmetry, and $^2A'_1$ electronic state. The optimized bond length 2.57 Å, is in good agreement with reported theoretical values 2.61 Å [6], 2.62 Å [7], 2.56 Å [19], and 2.52 Å [12, 13]. The doublet ground state is also confirmed with the results of magnetic deflection experiments [15].

The next isomer, which lies 0.83 eV high in energy, is isosceles triangular isomer. The optimized geometry has 2.59 Å, 2.59 Å and 2.99 Å as sides of triangle, with a quartet ground state (4A_2). Our results are in agreement with other theoretical results [7, 16, 19].

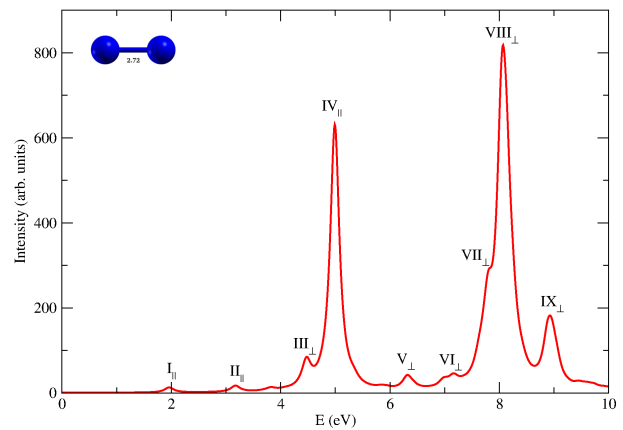


Figure 6: (Color online) The linear optical absorption spectrum of Al₂, calculated using the MRSDCI approach. The peaks corresponding to the light polarized along the molecular axis are labeled with the subscript \parallel , while those polarized perpendicular to it are denoted by the subscript \perp . For plotting the spectrum, a uniform linewidth of 0.1 eV was used.

Linear Al₃ isomer again with quartet multiplicity is the next low-lying isomer. The optimized bond length is 2.62 Å. This is in good agreement with few available reports [12, 16, 19].

The photoabsorption spectra of these isomers are presented in Figs. 7, 9 and 11. The corresponding many body wave functions of excited states corresponding to various peaks are presented in Table A.2, A.3 and A.4 respectively. In the equilateral triangular isomer, most of the intensity is concentrated at higher energies. The same is true for the isosceles triangular isomer. However, the spectrum of isosceles triangular isomer appears slightly red shifted with respect to the equilateral counterpart. Along with this shift, there appears a split pair

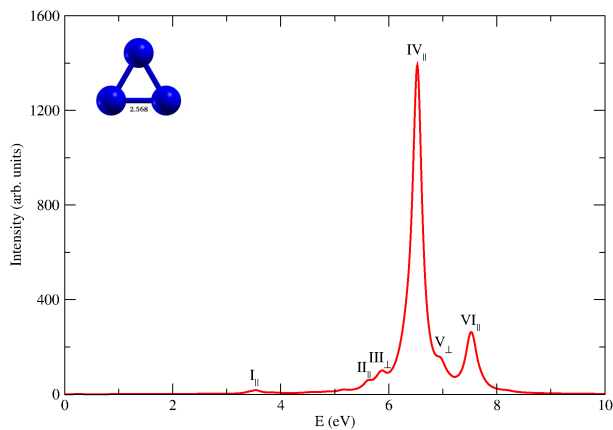


Figure 7: (Color online) The linear optical absorption spectrum of Al_3 equilateral triangle isomer, calculated using the MRSDCI approach. The peaks corresponding to the light polarized along the molecular plane are labeled with the subscript \parallel , while those polarized perpendicular to it are denoted by the subscript \perp . For plotting the spectrum, a uniform linewidth of 0.1 eV was used.

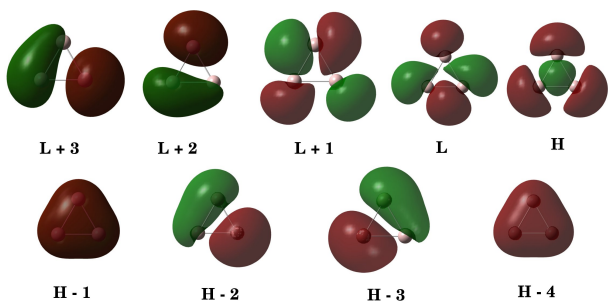


Figure 8: (Color online) Molecular orbitals of equilateral triangular aluminum trimer. H and L stands for HOMO and LUMO respectively.

of peaks at 5.8 eV. This splitting of oscillator strengths might be due to distortion accompanied by symmetry breaking. The absorption spectrum of linear isomer is altogether different with bulk of the oscillator strength carried by peaks in the range 4 – 5 eV, and, due to the polarization of light absorbed parallel to the axis of the trimer.

The optical absorption spectrum of equilateral triangular isomer consists of very feeble low energy peaks at 3.5 eV, 5.6 eV and 5.8 eV characterized by $H-3 \rightarrow L+5$, a double excitation $H-2 \rightarrow L+5$; $H-1 \rightarrow L+5$, and $H-3 \rightarrow L+2$ respectively. The latter peak is due to the light polarized perpendicular to the plane of the isomer. It is followed by an intense peak at around 6.5 eV with dominant contribution from $H \rightarrow L+6$ and $H \rightarrow L+4$ configurations. A semi-major peak is observed at 7.5 eV characterized mainly due to double excitations.

Two major peaks at 6.5 eV and 7.5 eV, obtained in our calculations are also found in the spectrum of TDLDA

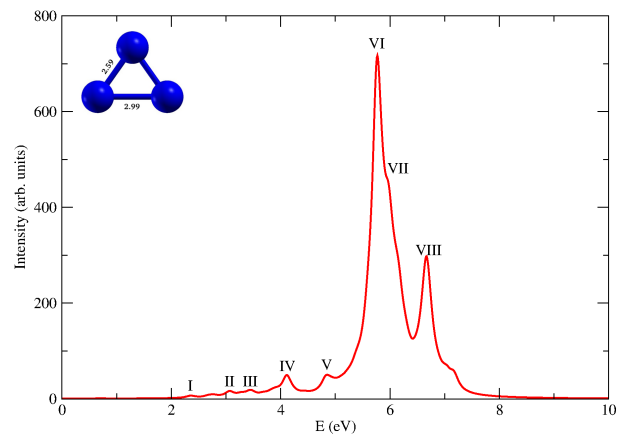


Figure 9: (Color online) The linear optical absorption spectrum of Al_3 isosceles triangle isomer, calculated using the MRSDCI approach. All peaks labeled above correspond to the light polarized along the molecular plane. For plotting the spectrum, a uniform linewidth of 0.1 eV was used.

calculations, with the difference that the latter does not have a smaller intensity in TDLDA [25]. Other major peaks obtained by Deshpande *et al.* [25] in the spectrum of aluminum trimer are not observed, or have very small intensity in our results.

As compared to the equilateral triangle spectra the isosceles triangular isomer exhibit several small intensity peaks (*cf.* Fig. 9) in the low energy regime. The majority of contribution to peaks of this spectrum comes from longitudinally polarized transitions, with negligible contribution from transverse polarized light. The spectrum starts with a feeble peak at 2.4 eV with contribution from doubly-excited configuration $H \rightarrow L+1$; $H-2 \rightarrow L+2$. One of the dominant contribution to the oscillator strength comes from two closely-lying peaks at 5.8 eV. The wave functions of excited states corresponding to this peak show a strong mixing of doubly-excited configurations, such as $H-3 \rightarrow L+1$; $H-2 \rightarrow L$ and $H-2 \rightarrow L+1$; $H-4 \rightarrow L$. The peak at 6.7 eV shows absorption mainly due to $H \rightarrow L+10$.

Linear trimer of aluminum cluster also shows low activity in the low energy range. Very feeble peaks are observed at 1.2 eV and 2.3 eV, both characterized by $H-3 \rightarrow H-2$. This configuration also contributes to the semi-major peak at 4 eV along with $H-4 \rightarrow H$. Two closely lying peaks at 4.3 eV and 4.6 eV carry the bulk of the oscillator strength. Major contribution to the former comes from $H-1 \rightarrow L+2$ along with $H-3 \rightarrow H-2$ being dominant in both the peaks. Again, as expected, the absorption due to light polarized along the trimer contributes substantially to the spectrum.

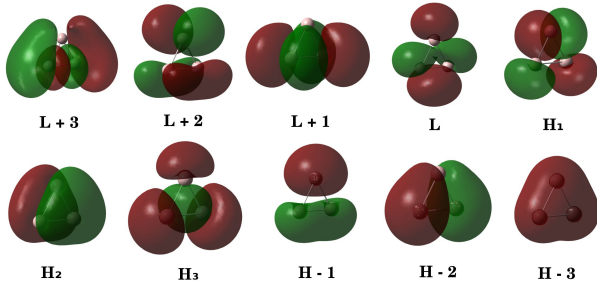


Figure 10: (Color online) Molecular orbitals of isosceles triangular aluminum trimer. H and L stands for HOMO and LUMO respectively, and H_1 , H_2 , and H_3 are singly occupied molecular orbitals.

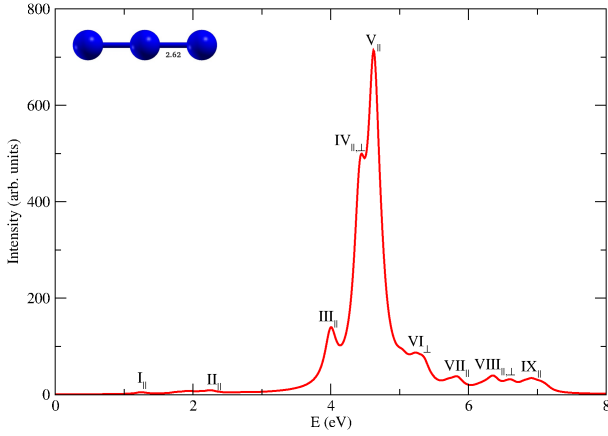


Figure 11: (Color online) The linear optical absorption spectrum of Al_3 linear isomer, calculated using the MRSDCI approach. The peaks corresponding to the light polarized along the molecular axis are labeled with the subscript \parallel , while those polarized perpendicular to it are denoted by the subscript \perp . For plotting the spectrum, a uniform linewidth of 0.1 eV was used.

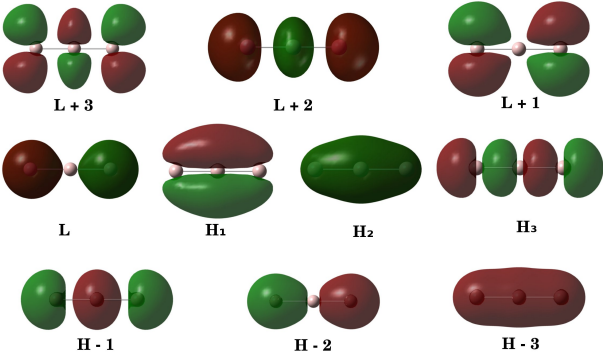


Figure 12: (Color online) Molecular orbitals of linear aluminum trimer. H and L stands for HOMO and LUMO respectively, and H_1 , H_2 , and H_3 are singly occupied molecular orbitals.

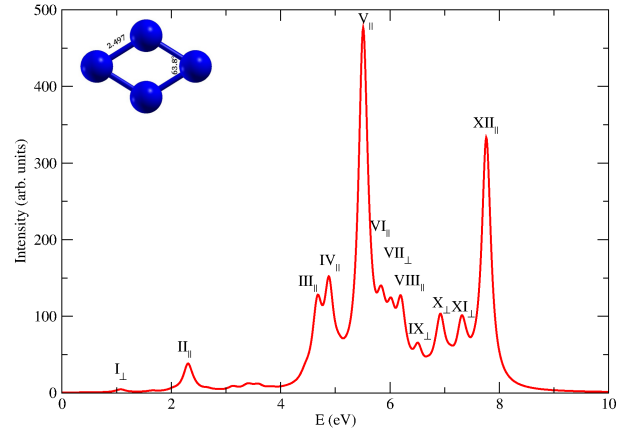


Figure 13: (Color online) The linear optical absorption spectrum of rhombus Al_4 , calculated using the MRSDCI approach. The peaks corresponding to the light polarized along the molecular axis are labeled with the subscript \parallel , while those polarized perpendicular to it are denoted by the subscript \perp . For plotting the spectrum, a uniform linewidth of 0.1 eV was used.

3. Al_4

Tetramer of aluminum cluster has many low lying isomers due to its flat potential energy curves. Among them, rhombus structure is the most stable with $^3B_{2g}$ electronic ground state. Our optimized bond length for rhombus structure is 2.50 Å and 63.8° as the acute angle. This is to be compared with corresponding reported values of 2.56 Å and 69.3° reported by Martinez *et al.* [19], 2.51 Å and 56.5° computed by Jones [17], 2.55 Å and 67.6° obtained by Schultz *et al.* [13]. We note that bond lengths are in good agreement but bond angles appear to vary a bit.

The other isomer studied here is an almost square shaped tetramer with optimized bond length of 2.69 Å. The electronic ground state of this D_{4h} symmetric cluster is $^3B_{3u}$. This optimized geometry is in accord with 2.69 Å reported by Martinez *et al.* [19], however it is somewhat bigger than 2.57 Å calculated by Yang *et al.* [12] and 2.61 Å obtained by Jones [16].

For planar clusters, like rhombus and square shaped Al_4 , two types of optical absorptions are possible: (a) Longitudinal – those polarized in the plane of the cluster, and (b) transverse – the ones polarized perpendicular to that plane. The onset of optical absorption in rhombus isomer occurs at around 1 eV with transversely polarized absorption characterized by $H_1 \rightarrow L + 1$. It is followed by an in-plane polarized absorption peak at 2.3 eV with dominant contribution from $H - 2 \rightarrow H_1$. Several closely lying peaks are observed in a small energy range of 4.5 – 8 eV. Peaks split from each other are seen in this range confirming that after shell closure, in perturbed droplet model, Jahn Teller distortion causes symmetry breaking usually associated with split absorption peaks. The most

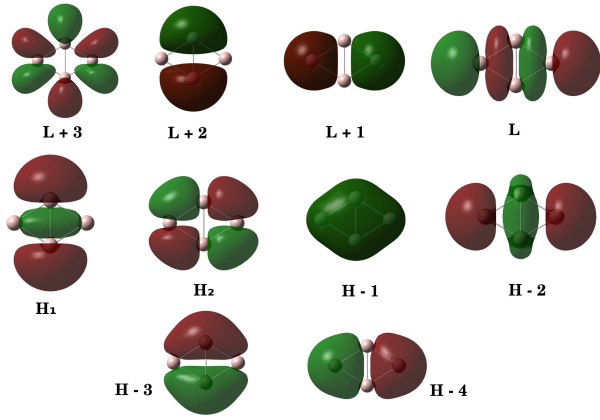


Figure 14: (Color online) Molecular orbitals of rhombus-shaped aluminum tetramer. H and L stands for HOMO and LUMO respectively, and H_1 and H_2 are singly occupied molecular orbitals.

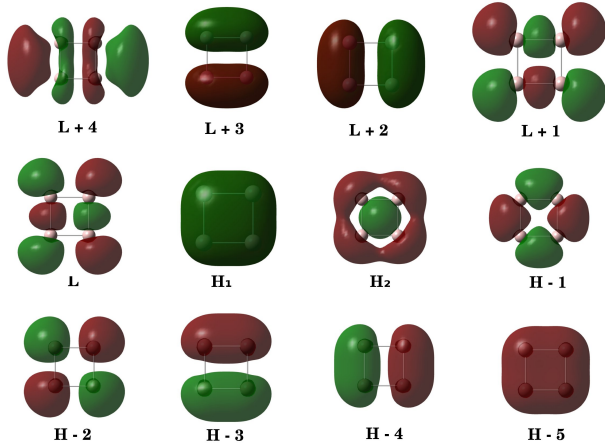


Figure 15: (Color online) Molecular orbitals of square-shaped aluminum tetramer. H and L stands for HOMO and LUMO respectively, and H_1 and H_2 are singly occupied molecular orbitals.

intense peak is observed at 5.5 eV characterized by $H - 3 \rightarrow L + 4$.

The absorption spectrum of square shaped isomer begins with a couple of low longitudinally polarized absorption peaks at 2.1 eV and 2.7 eV characterized by $H - 1 \rightarrow L$ and $H_2 \rightarrow L + 1$ respectively. The peak at 4.2 and 4.9 eV have $H - 2 \rightarrow L$ and $H_1 \rightarrow L + 2$ as respective dominant configurations. A major peak at 5.85 eV is observed with absorption due to longitudinal polarization having $H - 2 \rightarrow L + 2$ and a double excitation $H_1 \rightarrow L + 2; H - 2 \rightarrow L + 2$ as dominant configurations. These configurations also make dominant contribution to the peak at 6.5 eV. This peak along with one at 6.9 eV are two equally and most intense peaks of the spectrum. The latter has additional contribution from $H_1 \rightarrow L + 1; H - 2 \rightarrow L$. A shoulder peak is observed at 7.2 eV.

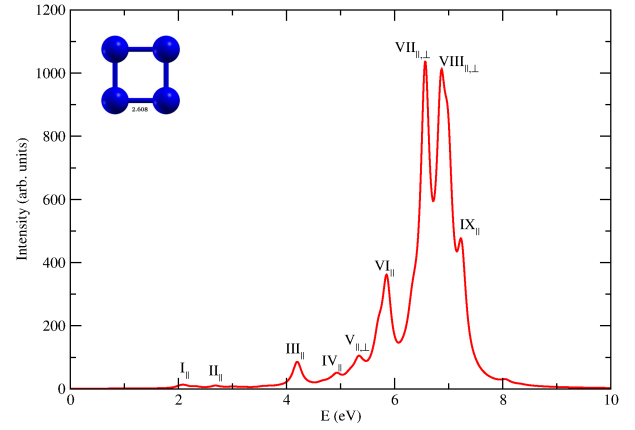


Figure 16: (Color online) The linear optical absorption spectrum of square Al_4 , calculated using the MRSDCI approach. The peaks corresponding to the light polarized along the molecular plane are labeled with the subscript \parallel , while those polarized perpendicular to it are denoted by the subscript \perp . For plotting the spectrum, a uniform linewidth of 0.1 eV was used.

The TDLDA spectrum [25] of aluminum rhombus tetramer is in very good agreement with our results. With a few exceptions of absence of small peaks in very low energy range, the spectrum matches very well with our spectrum. Peaks labeled III to XII in our calculated spectrum are also observed with TDLDA calculations, however, the relative intensity is not always found to be consistent. For example, the strongest absorption peak of TDLDA calculations, is at around 7.9 eV while we have observed a peak at this energy but with small intensity. Also the highest absorption peak in our calculations is at 5.5 eV, and TDLDA also reports a strong peak at the same energy [25].

4. Al_5

The lowest lying pentagon isomer of aluminum has C_{2v} symmetry and has an electronic ground state of 2A_1 . The bond lengths are as shown in Fig. 1(g). These are slightly bigger than those obtained by Rao and Jena [6] and Yang *et al.* [12] using the DFT approach. Many other reports have confirmed that the planar pentagon is the most stable isomer of Al_5 .

The other optimized structure of pentamer is perfect pyramid with C_{4v} symmetry and 2A_1 electronic ground state. This lies 0.76 eV above the global minimum structure. This is the only three dimensional structure studied in this paper for optical absorption. The optimized geometry is consistent with those reported earlier by Jones [16]. However, it should be noted that there exists many more similar or slightly distorted structure lying equally close to the global minimum.

The optical absorption spectrum of pentagonal Al_5 has

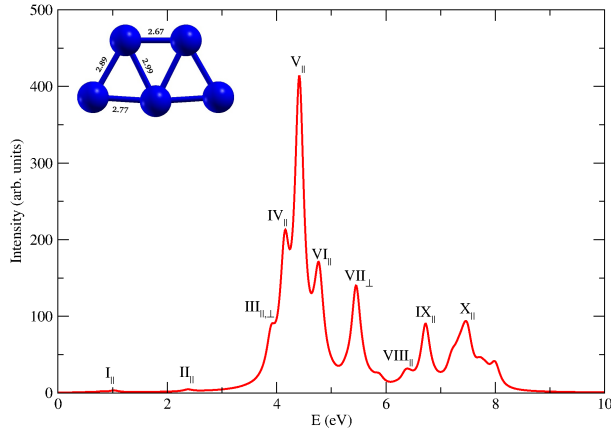


Figure 17: (Color online) The linear optical absorption spectrum of pentagonal Al_5 , calculated using the MRS-DCI approach. The peaks corresponding to the light polarized along the molecular axis are labeled with the subscript \parallel , while those polarized perpendicular to it are denoted by the subscript \perp . For plotting the spectrum, a uniform linewidth of 0.1 eV was used.

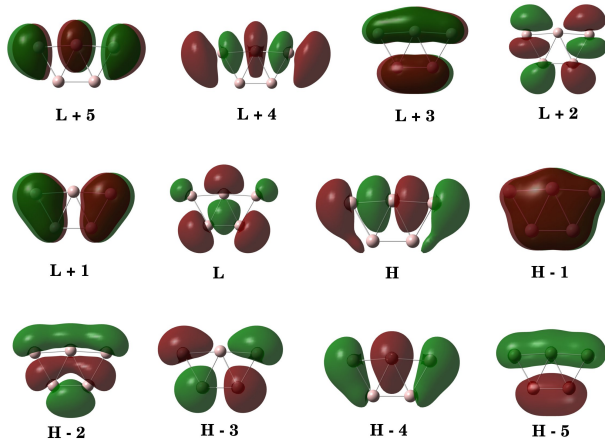


Figure 18: (Color online) Molecular orbitals of pentagonal aluminum pentamer. H and L stands for HOMO and LUMO respectively.

few low energy peaks followed by major absorption at 4.4 eV. It has dominant contribution from $H - 1 \rightarrow L + 5$ configuration. Pentagonal isomer shows more optical absorption in the high energy range, with peaks within regular intervals of energy.

Few feeble peaks occur in the low energy range in the optical absorption of pyramidal isomer. The major absorption peak at 4.2 eV is slightly red-shifted as compared to the pentagonal counterpart. It is characterized by $H - 3 \rightarrow L + 2$. A peak at 6 eV is seen in this absorption spectrum having dominant contribution from $H \rightarrow L + 13$, which is missing in the spectrum of pentagon. These differences can lead to identification of isomers produced experimentally.

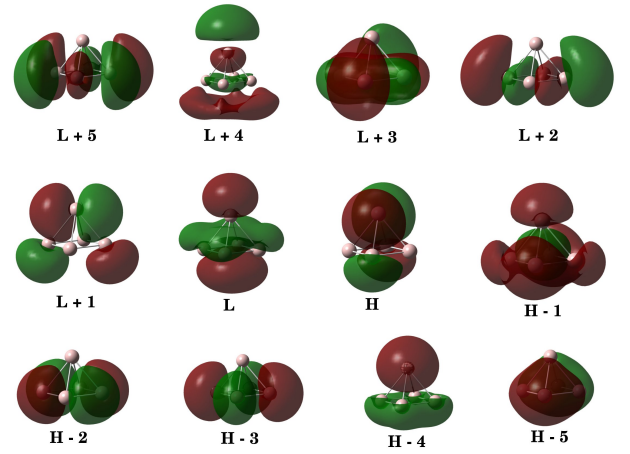


Figure 19: (Color online) Molecular orbitals of pyramidal aluminum pentamer. H and L stands for HOMO and LUMO respectively.

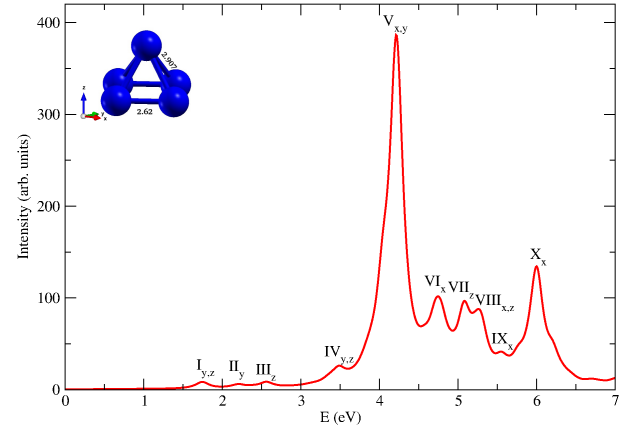


Figure 20: (Color online) The linear optical absorption spectrum of pyramidal Al_5 , calculated using the MRS-DCI approach. The peaks corresponding to the light polarized along the Cartesian axes are labeled accordingly. For plotting the spectrum, a uniform linewidth of 0.1 eV was used.

The TDLDA calculated spectrum [25] of pentagonal isomer is also in very good agreement with our results. A small peak at 2.4 eV is observed in both the spectra, followed by peaks at 3.9 eV, 4.2 eV and 4.4 eV. These three peaks are also observed in TDLDA results with a little bit of broadening. Again, the peak at 5.4 eV matches with each other calculated from both the approaches. Peak found at 6.7 eV is also observed using TDLDA calculation. In the range of spectrum studied in our calculations, the strongest peak position and intensity is in accord with that of TDLDA counterpart [25].

IV. CONCLUSIONS AND OUTLOOK

In this study, we have presented large-scale all-electron correlated calculations of optical absorption spectra of several low-lying isomers of aluminum clusters Al_n , ($n=2-5$). Both ground and excited state calculations were performed at MRSDCI level, which take electron correlations into account at a sophisticated level. We have analyzed the nature of low-lying excited states. Isomers of a given cluster show a distinct signature spectrum, indicating a strong-structure property relationship. This fact can be used in experiments to distinguish between different isomers of a cluster. Owing to sophistication of our calculations, our results can be used for benchmarking of the absorption spectra. The optical excitations involved are found to be collective type, and plasmonic in nature. This can also be used as another criterion for evolution of metallic character in metal atom clusters.

ACKNOWLEDGMENTS

The author (R.S.) would like to acknowledge the Council of Scientific and Industrial Research (CSIR), India, for research fellowship (09/087/(0600)2010-EMR-I).

Appendix A: Excited State CI Wavefunctions, Energies and Oscillator Strengths

In the following tables, we present the excitation energies (with respect to the ground state), the many body wavefunction and the oscillator strengths of the excited states corresponding to the peaks in the photoabsorption spectra of various isomers listed in Fig. 1, and discussed in section III.

Table A.1: Excitation energies (E) and many-particle wave functions of excited states corresponding to the peaks in the linear absorption spectrum of Al_2 (*cf.* Fig. 6), along with the oscillator strength (f_{12}) of the transitions.

Longitudinal and transverse polarization corresponds to the absorption due to light polarized along and perpendicular to the molecular axis respectively. In the wave function, the bracketed numbers are the CI coefficients of a given electronic configuration. Symbols H_1, H_2 denote SOMOs discussed earlier, and H , and L , denote HOMO and LUMO orbitals respectively. HF denotes the Hartree-Fock configuration.

| Peak | E (eV) | f_{12} | Polarization | Wave Function |
|-----------------|----------|----------|--------------|--|
| GS ^b | | | | $ H_1^1, H_2^1\rangle$ (0.9096) $ H - 1 \rightarrow H_1; H_2 \rightarrow L\rangle$ (0.1139) $ H - 2 \rightarrow L; H - 1 \rightarrow L + 2\rangle$ (0.0889) |
| I | 1.96 | 0.1027 | longitudinal | $ H_2 \rightarrow L + 1\rangle$ (0.8120) $ H - 1 \rightarrow H_1\rangle$ (0.3685) |
| II | 3.17 | 0.1249 | longitudinal | $ H - 1 \rightarrow H_1\rangle$ (0.6172) $ H_1 \rightarrow L + 3\rangle$ (0.4068) $ H_1 \rightarrow L; H - 1 \rightarrow L\rangle$ (0.3190) |
| III | 4.47 | 0.5149 | transverse | $ H_2 \rightarrow L + 4\rangle$ (0.8313) $ H_2 \rightarrow L + 6\rangle$ (0.2024) |
| IV | 4.99 | 5.4531 | longitudinal | $ H_1 \rightarrow L + 3\rangle$ (0.7353) $ H - 1 \rightarrow H_1\rangle$ (0.4104) |
| V | 6.31 | 0.2554 | transverse | $ H_2 \rightarrow L + 6\rangle$ (0.4683) $ H - 1 \rightarrow L + 1\rangle$ (0.3894) $ H - 1 \rightarrow L; H_2 \rightarrow L + 2\rangle$ (0.3886) |
| VI | 7.17 | 0.1549 | transverse | $ H_2 \rightarrow L + 2; H - 1 \rightarrow L\rangle$ (0.4782) $ H - 1 \rightarrow L + 1\rangle$ (0.4327) $ H_1 \rightarrow L; H_2 \rightarrow L + 8\rangle$ (0.3867) |
| VII | 7.79 | 1.2530 | transverse | $ H - 1 \rightarrow H_1; H_2 \rightarrow L + 3\rangle$ (0.4833) $ H_1 \rightarrow L + 7\rangle$ (0.3917) $ H_1 \rightarrow L; H_2 \rightarrow L + 8\rangle$ (0.3791) |
| VIII | 8.05 | 3.5391 | transverse | $ H - 2 \rightarrow L\rangle$ (0.5316) $ H - 1 \rightarrow L + 2\rangle$ (0.3756) $ H_1 \rightarrow L + 8\rangle$ (0.3531) |
| | 8.10 | 1.1418 | transverse | $ H - 1 \rightarrow H_1; H_2 \rightarrow L + 3\rangle$ (0.4788) $ H_2 \rightarrow L + 6\rangle$ (0.4095) |
| IX | 8.87 | 0.7044 | transverse | $ H_1 \rightarrow L + 11\rangle$ (0.5061) $ H_1 \rightarrow L; H_2 \rightarrow L + 7\rangle$ (0.4162) |
| | 8.95 | 0.6872 | transverse | $ H_1 \rightarrow L + 7\rangle$ (0.4932) $ H_2 \rightarrow L; H_1 \rightarrow L + 8\rangle$ (0.4414) $ H_1 \rightarrow L + 4; H - 1 \rightarrow L + 1\rangle$ (0.3262) |

^b GS does not correspond to any peak, rather it corresponds to the ground state wavefunction of Al_2 isomer.

Table A.2: Excitation energies (E) and many-particle wave functions of excited states corresponding to the peaks in the linear absorption spectrum of Al_3 equilateral triangle isomer (*cf.* Fig. 7), along with the oscillator strength (f_{12}) of the transitions. In-plane and transverse polarization corresponds to the absorption due to light polarized in and perpendicular to the plane of the triangular isomer respectively. In the wave function, the bracketed numbers are the CI coefficients of a given electronic configuration. Symbols H and L , denote HOMO (singly occupied, in this case) and LUMO orbitals respectively. HF denotes the Hartree-Fock configuration.

| Peak | E (eV) | f_{12} | Polarization | Wave Function |
|-----------------|----------|----------|--------------|--|
| GS ^c | | | | $ HF\rangle$ (0.8373) $ H - 2 \rightarrow L + 5\rangle$ (0.1329) |
| I | 3.42 | 0.0376 | in-plane | $ H - 3 \rightarrow L + 5\rangle$ (0.2908) $ H - 2 \rightarrow L + 1\rangle$ (0.2439) |
| | 3.54 | 0.1080 | in-plane | $ H - 2 \rightarrow L + 5\rangle$ (0.3686) $ H - 2 \rightarrow H\rangle$ (0.3403) |
| II | 5.61 | 0.2565 | in-plane | $ H - 2 \rightarrow L + 5; H - 1 \rightarrow L + 5\rangle$ (0.4854) $ H \rightarrow L + 1; H - 1 \rightarrow L + 1\rangle$ (0.4476) |
| III | 5.87 | 0.3413 | transverse | $ H - 3 \rightarrow L + 2\rangle$ (0.2915) $ H - 2 \rightarrow L\rangle$ (0.2842) |
| IV | 6.53 | 6.3289 | in-plane | $ H \rightarrow L + 6\rangle$ (0.4044) $ H - 3 \rightarrow L + 1\rangle$ (0.3965) |
| | 6.53 | 5.7925 | in-plane | $ H - 2 \rightarrow L + 5\rangle$ (0.3158) $ H \rightarrow L + 4\rangle$ (0.3842) $ H - 3 \rightarrow L + 5\rangle$ (0.2834) $ H - 4 \rightarrow L + 1\rangle$ (0.2256) |
| V | 6.96 | 0.4145 | transverse | $ H - 2 \rightarrow L\rangle$ (0.3140) $ H - 3 \rightarrow L + 2\rangle$ (0.2626) |
| VI | 7.50 | 0.9430 | in-plane | $ H - 2 \rightarrow L + 1; H \rightarrow L + 5\rangle$ (0.3136) $ H - 3 \rightarrow L + 5\rangle$ (0.2864) |
| | 7.57 | 0.8630 | in-plane | $ H \rightarrow L + 5; H - 3 \rightarrow L + 1\rangle$ (0.3838) $ H - 3 \rightarrow L + 1\rangle$ (0.2651) $ H - 2 \rightarrow L + 5\rangle$ (0.2590) |

^c GS does not correspond to any peak, rather it corresponds to the ground state wavefunction of Al_3 equilateral triangle isomer.

Table A.3: Excitation energies (E) and many-particle wave functions of excited states corresponding to the peaks in the linear absorption spectrum of Al_3 isosceles triangle isomer (*cf.* Fig. 9), along with the oscillator strength (f_{12}) of the transitions. In-plane and transverse polarization corresponds to the absorption due to light polarized in and perpendicular to the plane of the triangular isomer respectively. In the wave function, the bracketed numbers are the CI coefficients of a given electronic configuration. Symbols H_1 , H_2 and H_3 denote SOMOs discussed earlier, H and L , denote HOMO and LUMO orbitals respectively.

| Peak | E (eV) | f_{12} | Polarization | Wave Function |
|-----------------|----------|----------|--------------|---|
| GS ^d | | | | $ H_1^1, H_2^1, H_3^1\rangle$ (0.8670) $ H - 1 \rightarrow L + 10\rangle$ (0.1213) |
| I | 2.37 | 0.0358 | in-plane | $ H_1 \rightarrow L + 1; H_3 \rightarrow L + 2\rangle$ (0.7066) $ H - 1 \rightarrow L + 1; H_1 \rightarrow L\rangle$ (0.4052) |
| II | 3.06 | 0.0992 | in-plane | $ H_3 \rightarrow H_2; H - 2 \rightarrow L\rangle$ (0.4691) $ H - 1 \rightarrow L + 1; H_3 \rightarrow H_2\rangle$ (0.4070) |
| III | 3.45 | 0.0967 | in-plane | $ H_1 \rightarrow L + 3\rangle$ (0.5566) $ H - 1 \rightarrow L + 1; H_1 \rightarrow L\rangle$ (0.5209) |
| IV | 4.11 | 0.3208 | in-plane | $ H_1 \rightarrow L + 4\rangle$ (0.6038) $ H_3 \rightarrow L + 1; H - 2 \rightarrow L\rangle$ (0.5272) |
| V | 4.83 | 0.2242 | in-plane | $ H_1 \rightarrow L + 1; H - 2 \rightarrow L + 1\rangle$ (0.5321) $ H_1 \rightarrow L + 5\rangle$ (0.2611) |
| VI | 5.76 | 5.0792 | in-plane | $ H - 1 \rightarrow L + 1; H_3 \rightarrow L\rangle$ (0.3479) $ H - 3 \rightarrow L + 1; H_1 \rightarrow L\rangle$ (0.2875) $ H_2 \rightarrow L + 1; H_1 \rightarrow L + 3\rangle$ (0.2800) |
| | 5.85 | 0.8553 | in-plane | $ H_3 \rightarrow L + 1; H - 2 \rightarrow L\rangle$ (0.4081) $ H - 1 \rightarrow L; H_3 \rightarrow L\rangle$ (0.2400) |
| VII | 5.95 | 1.7094 | in-plane | $ H - 1 \rightarrow L + 2\rangle$ (0.3296) $ H - 1 \rightarrow L + 1; H_3 \rightarrow L\rangle$ (0.3138) |
| | 6.15 | 0.7827 | in-plane | $ H_1 \rightarrow L + 7\rangle$ (0.7827) |
| VIII | 6.68 | 1.7774 | in-plane | $ H_1 \rightarrow L + 10\rangle$ (0.4548) $ H_2 \rightarrow L + 1; H_1 \rightarrow L + 6\rangle$ (0.2705) $ H_1 \rightarrow L + 6\rangle$ (0.2447) |

^d GS does not correspond to any peak, rather it corresponds to the ground state wavefunction of Al_3 isosceles triangle isomer.

Table A.4: Excitation energies (E) and many-particle wave functions of excited states corresponding to the peaks in the linear absorption spectrum of Al_3 linear isomer (*cf.* Fig. 11), along with the oscillator strength (f_{12}) of the transitions. Longitudinal and transverse polarization corresponds to the absorption due to light polarized along and perpendicular to the axis of the linear isomer respectively. In the wave function, the bracketed numbers are the CI coefficients of a given electronic configuration. Symbols H_1 , H_2 and H_3 denote SOMOs discussed earlier, H and L , denote HOMO and LUMO orbitals respectively. HF denotes the Hartree-Fock configuration.

| Peak | E (eV) | f_{12} | Polarization | Wave Function |
|-----------------|----------|----------|--------------|---|
| GS ^e | | | | $ H_1^1, H_2^1, H_3^1\rangle$ (0.8010) $ H - 3 \rightarrow H - 1; H - 2 \rightarrow L\rangle$ (0.1913) |
| I | 1.24 | 0.0317 | longitudinal | $ H_2 \rightarrow L + 1\rangle$ (0.6602) $ H - 1 \rightarrow H_3\rangle$ (0.3636) |
| II | 2.25 | 0.0489 | longitudinal | $ H - 1 \rightarrow H_3\rangle$ (0.6856) $ H - 2 \rightarrow H_1\rangle$ (0.3230) |
| III | 4.01 | 0.9019 | longitudinal | $ H - 2 \rightarrow H_1\rangle$ (0.5249) $ H - 1 \rightarrow H_3\rangle$ (0.3471) |
| IV | 4.43 | 2.8593 | longitudinal | $ H - 1 \rightarrow H_3\rangle$ (0.4070) $ H - 1 \rightarrow L + 4; H_2 \rightarrow L + 6\rangle$ (0.2409) |
| | 4.47 | 0.0960 | transverse | $ H_2 \rightarrow L + 2\rangle$ (0.5402) $ H - 1 \rightarrow H_3; H_2 \rightarrow L + 6\rangle$ (0.3068) |
| V | 4.62 | 5.1747 | longitudinal | $ H - 1 \rightarrow H_3\rangle$ (0.4600) $ H - 1 \rightarrow L + 4; H_2 \rightarrow L + 6\rangle$ (0.2862) |
| VI | 5.29 | 0.1070 | transverse | $ H_2 \rightarrow L + 5\rangle$ (0.4951) $ H - 1 \rightarrow H_3; H - 1 \rightarrow L + 1\rangle$ (0.3284) $ H - 1 \rightarrow L + 3\rangle$ (0.3091) |
| VII | 5.83 | 0.1412 | longitudinal | $ H - 1 \rightarrow L + 2; H_1 \rightarrow L\rangle$ (0.6637) $ H - 2 \rightarrow H_1\rangle$ (0.2225) $ H - 1 \rightarrow H_3\rangle$ (0.2073) |
| VIII | 6.31 | 0.0459 | longitudinal | $ H_1 \rightarrow L + 6; H_3 \rightarrow L\rangle$ (0.5099) $ H_1 \rightarrow L; H_3 \rightarrow L + 6\rangle$ (0.2706) |
| | 6.37 | 0.0740 | transverse | $ H - 1 \rightarrow L + 3\rangle$ (0.3989) $ H - 1 \rightarrow H_2; H_3 \rightarrow L + 6\rangle$ (0.2266) |
| IX | 6.89 | 0.1311 | longitudinal | $ H - 5 \rightarrow L + 6\rangle$ (0.3920) $ H_1 \rightarrow L + 4; H_3 \rightarrow L + 6\rangle$ (0.3086) |

^e GS does not correspond to any peak, rather it corresponds to the ground state wavefunction of Al_3 linear triangle isomer.

Table A.5: Excitation energies (E) and many-particle wave functions of excited states corresponding to the peaks in the linear absorption spectrum of Al₄ rhombus isomer (*cf.* Fig. 13), along with the oscillator strength (f_{12}) of the transitions. In-plane and transverse polarization corresponds to the absorption due to light polarized in and perpendicular to the plane of the rhombus isomer respectively. In the wave function, the bracketed numbers are the CI coefficients of a given electronic configuration. Symbols H_1, H_2 denote SOMOs discussed earlier, and H , and L , denote HOMO and LUMO orbitals respectively.

| Peak | E (eV) | f_{12} | Polarization | Wave Function |
|-----------------|----------|----------|--------------|--|
| GS ^f | | | | $ H_1^1, H_2^1\rangle$ (0.8724) $ H - 3 \rightarrow L; H - 3 \rightarrow L\rangle$ (0.1050) |
| I | 1.07 | 0.0247 | transverse | $ H_1 \rightarrow L + 1\rangle$ (0.8489) $ H - 2 \rightarrow L + 5\rangle$ (0.1601) |
| II | 2.31 | 0.3087 | in-plane | $ H - 2 \rightarrow H_1\rangle$ (0.7645) $ H_2 \rightarrow L + 1\rangle$ (0.3113) |
| III | 4.67 | 0.5709 | in-plane | $ H - 2 \rightarrow L; H - 1 \rightarrow L + 3\rangle$ (0.6036) $ H - 1 \rightarrow L + 3\rangle$ (0.4213) $ H_1 \rightarrow L + 7\rangle$ (0.3113) |
| IV | 4.88 | 0.9622 | in-plane | $ H - 1 \rightarrow L; H - 1 \rightarrow L + 3\rangle$ (0.6036) $ H - 3 \rightarrow L\rangle$ (0.4699) |
| V | 5.51 | 3.8316 | in-plane | $ H - 3 \rightarrow L + 4\rangle$ (0.7378) $ H - 2 \rightarrow H_1\rangle$ (0.2161) |
| VI | 5.84 | 0.4900 | in-plane | $ H - 2 \rightarrow L + 3\rangle$ (0.3889) $ H - 2 \rightarrow L; H - 3 \rightarrow L\rangle$ (0.3758) $ H - 3 \rightarrow L\rangle$ (0.3594) $ H - 1 \rightarrow L; H - 1 \rightarrow L + 3\rangle$ (0.3591) |
| VII | 6.01 | 0.5332 | transverse | $ H_2 \rightarrow L + 7\rangle$ (0.7268) $ H - 3 \rightarrow L + 2\rangle$ (0.3050) |
| VIII | 6.20 | 0.7477 | in-plane | $ H - 2 \rightarrow L + 3\rangle$ (0.5195) $ H - 2 \rightarrow L; H - 3 \rightarrow L\rangle$ (0.4189) |
| IX | 6.51 | 0.2928 | transverse | $ H - 3 \rightarrow L + 2\rangle$ (0.7001) $ H - 2 \rightarrow H_1; H - 1 \rightarrow L + 2\rangle$ (0.2232) $ H - 2 \rightarrow L; H - 3 \rightarrow L + 2\rangle$ (0.2070) |
| X | 6.92 | 0.6053 | transverse | $ H - 3 \rightarrow L + 2\rangle$ (0.5144) $ H - 2 \rightarrow L; H - 3 \rightarrow L + 2\rangle$ (0.3549) $ H - 2 \rightarrow L + 5\rangle$ (0.2676) |
| XI | 7.31 | 0.4328 | transverse | $ H - 2 \rightarrow L + 5\rangle$ (0.4033) $ H - 3 \rightarrow L; H - 1 \rightarrow L + 1\rangle$ (0.3787) |
| XII | 7.76 | 2.7450 | in-plane | $ H_1 \rightarrow L + 8\rangle$ (0.4387) $ H_1 \rightarrow L + 1; H - 1 \rightarrow L + 2\rangle$ (0.3435) |

^f GS does not correspond to any peak, rather it corresponds to the ground state wavefunction of Al₄ rhombus isomer.

Table A.6: Excitation energies (E) and many-particle wave functions of excited states corresponding to the peaks in the linear absorption spectrum of Al_4 square isomer (*cf.* Fig. 16), along with the oscillator strength (f_{12}) of the transitions. In-plane and transverse polarization corresponds to the absorption due to light polarized in and perpendicular to the plane of the rhombus isomer respectively. In the wave function, the bracketed numbers are the CI coefficients of a given electronic configuration. Symbols H_1, H_2 denote SOMOs discussed earlier, and H , and L , denote HOMO and LUMO orbitals respectively.

| Peak | E (eV) | f_{12} | Polarization | Wave Function |
|-----------------|----------|----------|--------------|---|
| GS ^g | | | | $ H_1^1, H_2^1\rangle(0.8525)$ $ H_1 \rightarrow L; H - 2 \rightarrow L\rangle(0.0972)$ |
| I | 2.08 | 0.0278 | in-plane | $ H - 1 \rightarrow L\rangle(0.7191)$ $ H - 1 \rightarrow H_1; H_2 \rightarrow L + 1\rangle(0.2645)$ $ H_2 \rightarrow L + 1\rangle(0.2536)$ $ H_1 \rightarrow L\rangle(0.2443)$ |
| II | 2.68 | 0.0301 | in-plane | $ H_2 \rightarrow L + 1\rangle(0.4757)$ $ H - 1 \rightarrow L\rangle(0.4358)$ $ H - 1 \rightarrow H_1; H_2 \rightarrow L + 1\rangle(0.3608)$ |
| III | 4.19 | 0.3420 | in-plane | $ H - 2 \rightarrow L\rangle(0.5889)$ $ H - 1 \rightarrow L + 2\rangle(0.4283)$ $ H_1 \rightarrow L\rangle(0.2329)$ |
| IV | 4.92 | 0.1131 | in-plane | $ H_1 \rightarrow L + 2\rangle(0.5780)$ $ H - 1 \rightarrow L + 2\rangle(0.4083)$ $ H - 2 \rightarrow L\rangle(0.3198)$ |
| V | 5.17 | 0.1238 | transverse | $ H - 2 \rightarrow L; H_1 \rightarrow L + 1\rangle(0.3693)$ $ H - 2 \rightarrow L; H_1 \rightarrow L + 1\rangle(0.3692)$ |
| | 5.33 | 0.2470 | in-plane | $ H - 2 \rightarrow H_1; H - 2 \rightarrow L\rangle(0.5193)$ $ H - 1 \rightarrow L + 2\rangle(0.3915)$ $ H - 2 \rightarrow L + 2\rangle(0.3335)$ |
| VI | 5.85 | 1.2446 | in-plane | $ H - 2 \rightarrow L + 2\rangle(0.7184)$ $ H - 1 \rightarrow H_1; H - 2 \rightarrow L + 2\rangle(0.2587)$ $ H - 1 \rightarrow L + 2\rangle(0.2579)$ |
| VII | 6.55 | 3.7894 | in-plane | $ H - 2 \rightarrow L + 2\rangle(0.5706)$ $ H - 1 \rightarrow H_1; H - 2 \rightarrow L + 2\rangle(0.4089)$ $ H - 1 \rightarrow L + 2\rangle(0.3325)$ |
| | 6.58 | 0.2634 | transverse | $ H_1 \rightarrow L + 1; H - 2 \rightarrow L\rangle(0.4375)$ $ H_1 \rightarrow L + 1; H - 2 \rightarrow L\rangle(0.4375)$ $ H - 2 \rightarrow L + 3\rangle(0.4183)$ |
| VIII | 6.87 | 2.9702 | in-plane | $ H - 2 \rightarrow L + 2\rangle(0.5100)$ $ H - 1 \rightarrow L + 2\rangle(0.3495)$ |
| | 6.93 | 0.2483 | transverse | $ H_1 \rightarrow L + 1; H - 2 \rightarrow L\rangle(0.3558)$ $ H_1 \rightarrow L + 1; H - 2 \rightarrow L\rangle(0.3558)$ $ H - 2 \rightarrow L + 3\rangle(0.2929)$ |
| IX | 7.22 | 1.4267 | in-plane | $ H - 1 \rightarrow H_1; H - 2 \rightarrow L + 2\rangle(0.4039)$ $ H - 3 \rightarrow H_1\rangle(0.2900)$ $ H - 1 \rightarrow H_1; H - 1 \rightarrow L + 2\rangle(0.2848)$ |

^g GS does not correspond to any peak, rather it corresponds to the ground state wavefunction of Al_4 square isomer.

Table A.7: Excitation energies (E) and many-particle wave functions of excited states corresponding to the peaks in the linear absorption spectrum of Al_5 pentagon isomer (*cf.* Fig. 17), along with the oscillator strength (f_{12}) of the transitions. In-plane and transverse polarization corresponds to the absorption due to light polarized in and perpendicular to the plane of the pentagon isomer respectively. In the wave function, the bracketed numbers are the CI coefficients of a given electronic configuration. Symbols H and L , denote HOMO and LUMO orbitals respectively.

| Peak | E (eV) | f_{12} | Polarization | Wave Function |
|-----------------|----------|----------|--------------|--|
| GS ^h | | | | $ (H-2)^1\rangle (0.8679)$ $ H-2 \rightarrow L+1; H \rightarrow L+2\rangle (0.1045)$ |
| I | 1.03 | 0.0195 | in-plane | $ H-1 \rightarrow L\rangle (0.8635)$ $ H-1 \rightarrow L; H \rightarrow L+3\rangle (0.0880)$ |
| II | 2.38 | 0.0219 | in-plane | $ H-3 \rightarrow H-2\rangle (0.8560)$ $ H-1 \rightarrow L+4\rangle (0.1387)$ |
| III | 3.90 | 0.1042 | transverse | $ H \rightarrow L+4\rangle (0.8387)$ $ H \rightarrow L; H-1 \rightarrow L+2\rangle (0.1944)$ |
| | | 0.3362 | in-plane | $ H-4 \rightarrow L\rangle (0.8140)$ $ H-2 \rightarrow L+9\rangle (0.1841)$ |
| IV | 4.16 | 1.3144 | in-plane | $ H-1 \rightarrow L+4\rangle (0.7276)$ $ H-1 \rightarrow L+5\rangle (0.4478)$ |
| V | 4.42 | 3.3339 | in-plane | $ H-1 \rightarrow L+5\rangle (0.7096)$ $ H-1 \rightarrow L+4\rangle (0.4490)$ $ H-1 \rightarrow L+9\rangle (0.1535)$ |
| VI | 4.78 | 1.0471 | in-plane | $ H-2 \rightarrow L+9\rangle (0.7992)$ $ H-2 \rightarrow L; H \rightarrow L+6\rangle (0.2058)$ |
| VII | 5.46 | 1.1014 | transverse | $ H \rightarrow L+13\rangle (0.8156)$ $ H \rightarrow L; H-2 \rightarrow L\rangle (0.1708)$ |
| VIII | 6.37 | 0.1270 | in-plane | $ H-3 \rightarrow L\rangle (0.7632)$ |
| IX | 6.73 | 0.7104 | in-plane | $ H-3 \rightarrow L\rangle (0.7370)$ $ H \rightarrow L+1\rangle (0.3698)$ $ H-1 \rightarrow L; H \rightarrow L+3\rangle (0.1225)$ |
| X | 7.49 | 0.3989 | in-plane | $ H \rightarrow L+3\rangle (0.5087)$ $ H-2 \rightarrow L+16\rangle (0.3508)$ $ H \rightarrow L; H-1 \rightarrow L+1\rangle (0.2937)$ |

^h GS does not correspond to any peak, rather it corresponds to the ground state wavefunction of Al_5 pentagon isomer.

Table A.8: Excitation energies (E) and many-particle wave functions of excited states corresponding to the peaks in the linear absorption spectrum of Al_5 pyramid isomer (*cf.* Fig. 20), along with the oscillator strength (f_{12}) of the transitions. In the wave function, the bracketed numbers are the CI coefficients of a given electronic configuration. Symbols H and L , denote HOMO and LUMO orbitals respectively.

| Peak | E (eV) | f_{12} | Polarization | Wave Function |
|-----------------|----------|----------|--------------|--|
| GS ⁱ | | | | $ (H-2)^1\rangle$ (0.8591) $ H-3 \rightarrow L+1; H-3 \rightarrow L+1\rangle$ (0.1138) |
| I | 1.72 | 0.0046 | y | $ H-3 \rightarrow L+1\rangle$ (0.6849) |
| | 1.75 | 0.0521 | z | $ H-2 \rightarrow L+1\rangle$ (0.2887) $ H \rightarrow L+3\rangle$ (0.2887) |
| II | 2.21 | 0.0296 | y | $ H-3 \rightarrow L+1\rangle$ (0.7170) $ H-2 \rightarrow L+2\rangle$ (0.3402) $ H-3 \rightarrow L+2\rangle$ (0.2290) |
| III | 2.55 | 0.0477 | z | $ H \rightarrow L+3\rangle$ (0.5390) $ H-4 \rightarrow H-2\rangle$ (0.1296) |
| IV | 3.46 | 0.0399 | y | $ H-3 \rightarrow L; H-2 \rightarrow L+1\rangle$ (0.6131) |
| | 3.48 | 0.0769 | z | $ H-3 \rightarrow L+2\rangle$ (0.4975) $ H-4 \rightarrow H-2\rangle$ (0.7340) $ H-4 \rightarrow L\rangle$ (0.3735) |
| V | 4.04 | 0.6432 | x | $ H \rightarrow L+7\rangle$ (0.5929) $ H \rightarrow L+4\rangle$ (0.4432) |
| | 4.22 | 3.0735 | y | $ H-3 \rightarrow L+2\rangle$ (0.8272) $ H-3 \rightarrow L+1\rangle$ (0.1580) |
| VI | 4.74 | 0.3474 | x | $ H \rightarrow L\rangle$ (0.7617) $ H \rightarrow L+7\rangle$ (0.2542) |
| VII | 5.08 | 0.5494 | z | $ H-2 \rightarrow L; H \rightarrow L+2\rangle$ (0.5540) $ H-4 \rightarrow L\rangle$ (0.4833) |
| VIII | 5.26 | 0.3175 | z | $ H-2 \rightarrow L; H \rightarrow L+5\rangle$ (0.6251) $ H-4 \rightarrow L\rangle$ (0.3902) |
| | 5.27 | 0.1267 | x | $ H-6 \rightarrow H-2; H \rightarrow L+1\rangle$ (0.6056) $ H \rightarrow L\rangle$ (0.3242) |
| IX | 5.56 | 0.1384 | x | $ H \rightarrow L+11\rangle$ (0.7819) $ H \rightarrow L+13\rangle$ (0.3051) |
| X | 6.00 | 1.0052 | x | $ H \rightarrow L+13\rangle$ (0.8132) $ H \rightarrow L+11\rangle$ (0.1852) |

ⁱ GS does not correspond to any peak, rather it corresponds to the ground state wavefunction of Al_5 pyramid isomer.

-
- [1] J. A. Alonso, *Structure and Properties of Atomic Nanostructures* (Imperial College Press, London, 2005).
- [2] T. K. Yoshiyuki Kawazoe and K. Ohno, *Clusters and Nanomaterials* (Springer-Verlag, Berlin, 2002).
- [3] J. Jellinek, *Theory of Atomic and Molecular Clusters – With a Glimpse at Experiments* (Springer-Verlag, Berlin, 1999).
- [4] W. A. de Heer, *Rev. Mod. Phys.* **65**, 611 (1993).
- [5] J. Bownan, A. Liang, and W. A. de Heer, *Phys. Rev. Lett.* **106**, 043401 (2011).
- [6] B. K. Rao and P. Jena, *J. Chem. Phys.* **111**, 1890 (1999).
- [7] T. H. Upton, *J. Chem. Phys.* **86**, 7054 (1987).
- [8] K. Clemenger, *Phys. Rev. B* **32**, 1359 (1985).
- [9] G. Ganteför and W. Eberhardt, *Chem. Phys. Lett.* **217**, 600 (1994).
- [10] X. Li, H. Wu, X.-B. Wang, and L.-S. Wang, *Phys. Rev. Lett.* **81**, 1909 (1998).
- [11] R. Ahlrichs and S. D. Elliott, *Phys. Chem. Chem. Phys.* **1**, 13 (1999).
- [12] S. H. Yang, D. A. Drabold, J. B. Adams, and A. Sachdev, *Phys. Rev. B* **47**, 1567 (1993).
- [13] N. E. Schultz, G. Staszewska, P. Staszewski, and D. G. Truhlar, *J. Phys. Chem. B* **108**, 4850 (2004).
- [14] H.-P. Cheng, R. S. Berry, and R. L. Whetten, *Phys. Rev. B* **43**, 10647 (1991).
- [15] D. M. Cox, D. J. Trevor, R. L. Whetten, E. A. Rohlfing, and A. Kaldor, *J. Chem. Phys.* **84**, 4651 (1986).
- [16] R. O. Jones, *J. Chem. Phys.* **99**, 1194 (1993).
- [17] R. O. Jones, *Phys. Rev. Lett.* **67**, 224 (1991).
- [18] J. Akola, H. Häkkinen, and M. Manninen, *Phys. Rev. B* **58**, 3601 (1998).
- [19] A. Martinez, A. Vela, D. R. Salahub, P. Calaminici, and N. Russo, *J. Chem. Phys.* **101**, 10677 (1994).
- [20] M. Alipour and A. Mohajeri, *J. Phys. Chem. A* **114**, 12709 (2010).
- [21] J. M. Pacheco and J. L. Martins, *J. Chem. Phys.* **106**, 6039 (1997).
- [22] Pal, G., Pavlyukh, Y., Hübner, W., and Schneider, H. C., *Eur. Phys. J. B* **79**, 327 (2011).
- [23] C. R. C. Wang, S. Pollack, D. Cameron, and M. M. Kappes, *J. Chem. Phys.* **93**, 3787 (1990).
- [24] K. Selby, V. Kresin, J. Masui, M. Vollmer, W. A. de Heer, A. Scheidemann, and W. D. Knight, *Phys. Rev. B* **43**, 4565 (1991).
- [25] M. D. Deshpande, D. G. Kanhere, I. Vasiliev, and R. M. Martin, *Phys. Rev. B* **68**, 035428 (2003).
- [26] R.-H. Xie, G. W. Bryant, J. Zhao, T. Kar, and V. H. Smith, *Phys. Rev. B* **71**, 125422 (2005).
- [27] R. Shinde and A. Shukla, *Nano LIFE* **2**, 1240004 (2012).
- [28] M. J. Frisch, G. W. Trucks, H. B. Schlegel, G. E. Scuseria, M. A. Robb, J. R. Cheeseman, G. Scalmani, V. Barone, B. Mennucci, G. A. Petersson, H. Nakatsuji, M. Caricato, X. Li, H. P. Hratchian, A. F. Izmaylov, J. Bloino, G. Zheng, J. L. Sonnenberg, M. Hada, M. Ehara, K. Toyota, R. Fukuda, J. Hasegawa, M. Ishida, T. Nakajima, Y. Honda, O. Kitao, H. Nakai, T. Vreven, J. A. Montgomery, Jr., J. E. Peralta, F. Ogliaro, M. Bearpark, J. J. Heyd, E. Brothers, K. N. Kudin, V. N. Staroverov, R. Kobayashi, J. Normand, K. Raghavachari, A. Rendell, J. C. Burant, S. S. Iyengar, J. Tomasi, M. Cossi, N. Rega, J. M. Millam, M. Klene, J. E. Knox, J. B. Cross, V. Bakken, C. Adamo, J. Jaramillo, R. Gomperts, R. E. Stratmann, O. Yazyev, A. J. Austin, R. Cammi, C. Pomelli, J. W. Ochterski, R. L. Martin, K. Morokuma, V. G. Zakrzewski, G. A. Voth, P. Salvador, J. J. Dannenberg, S. Dapprich, A. D. Daniels, Å. Farkas, J. B. Foresman, J. V. Ortiz, J. Cioslowski, and D. J. Fox, “Gaussian 09 Revision A.02,” Gaussian Inc. Wallingford CT 2009.
- [29] L. E. McMurchie, S. T. Elbert, S. R. Langhoff, and E. R. Davidson, MELD package from Indiana University. It has been modified by us to handle bigger systems.
- [30] P. Sony and A. Shukla, *J. Chem. Phys.* **131**, 014302 (2009).
- [31] A. Shukla, *Phys. Rev. B* **65**, 125204 (2002).
- [32] P. Sony and A. Shukla, *Phys. Rev. B* **71**, 165204 (2005).
- [33] P. Sony and A. Shukla, *Phys. Rev. B* **75**, 155208 (2007).
- [34] K. L. Schuchardt, B. T. Didier, T. Elsethagen, L. Sun, V. Gurumoorthi, J. Chase, J. Li, and T. L. Windus, *J. Chem. Inf. Model.* **47**, 1045 (2007).
- [35] D. Feller, *J. Comput. Chem.* **17**, 1571 (1996).
- [36] O. Lehtonen, D. Sundholm, R. Send, and M. P. Johansson, *J. Chem. Phys.* **131**, 024301 (2009).
- [37] A. Szabo and N. Ostlund, *Modern Quantum Chemistry : Introduction to Advanced Electronic Structure Theory* (Dover Publications, New York, 1996).
- [38] J. Charles W. Bauschlicher, H. Partridge, S. R. Langhoff, P. R. Taylor, and S. P. Walch, *J. Chem. Phys.* **86**, 7007 (1987).
- [39] M. Cai, T. Dzugan, and V. Bondybey, *Chem. Phys. Lett.* **155**, 430 (1989).